Threading Dislocations in GaN HEMTs on Silicon: Origin of Large Time Constant Transients?

Saptarsi Ghosh*, Ankush Bag, Partha Mukhapadhay, Syed Mukulika Dinara,
Sanjay K. Jana, Sanjib Kabi, and Dhrubes Biswas

Advanced Technology Development Centre, Indian Institute of Technology Kharagpur
Kharagpur-721302, W.B., INDIA. ***Phone: (+91)9836385365 E-mail: saptarsi123@gmail.com**

KEYWORDS: **GaN HEMTs, TDDs, current collapse, transient, traps.**

Abstract

The possibility of threading dislocations affecting the frequency performance is explored through HEMTs having dislocation density orders apart. Pulsed I-V measurements show severe compression for the HEMTs grown on silicon. Analyzing the slow detrapping transients, a trapping process with time constant in the order of seconds could be identified for these same HEMTs. The absence of both trapping processes of such nature and current collapse were observed for HEMTs grown on sapphire. Our findings unambiguously correlate extent of slow transients in GaN HEMTs on silicon with threading dislocation density.

INTRODUCTION

Even with promising attributes such as high mobility, wide bandgap, high saturation velocity, high breakdown field, and polarization induced high sheet charge density; III-nitride systems still have a number of barriers to surpass before they can be implemented for reliable high frequency power performances. The significant decrease in microwave power output of GaN/AlGaN(or InAlN) HEMTs from the predicted DC load line curves is distinguished by current dispersion/slump [1]; a phenomenon exemplifying increase in knee voltage and decrease in the maximum channel current at pulsed biases. Electrically active traps held responsible for such collapse can be distributed anywhere in the band gap, and give rise to corresponding slow/fast transients. The response of an active trap with respect to an external stimulus (e.g. voltage pulse) is dependent on the emission/capture time constants of the carriers (electrons or holes) which in turn vary exponentially with the position of the trap in the bandgap. Thus traps located deep inside the bandgap should give rise to slow transients and severe current collapse.

On the other hand, role of dislocations in nitride devices has been a topic of numerous debates. There have been contradictory arguments regarding the effect of dislocations on the luminescence intensity of LEDs and on the leakage currents in Schottky diodes [2, 3]. In contrast, the correlation of dislocations and transient characteristics has rarely been investigated [4]. Several self-consistent density functional calculations and other empirical potential based approaches have theoretically suggested that dislocations induce deep levels according to the stoichiometry of the dislocation core, coordination of atoms, and strain fields around the core [5]. In such a case, discrete deep states arising from dislocations should give rise to slow transients with electron emission time constants in the order of seconds. Also, as the density of trap states is proportional to the threading dislocation density, hence identical structures with different TDDs should demonstrate different transient response and current collapse. In order to explore this phenomenon, we have analyzed two GaN/AlGaN based HEMTs having dislocation density two orders apart to investigate whether the transient and pulse characteristics are affected proportionately. The outcome should cause epitaxial engineers to strategize their growth accordingly on inexpensive silicon substrates which generate high dislocation density in active epi-layers. This will ensure bulk commercialization of GaN-HEMT-on-Si technology in the form of RF power amplifier and switches, replacing the present leaders, III-As based HBTs and p-HEMTs which fall quite short in terms of the power performance offered by III-Nitrides.

EXPERIMENTAL DETAILS AND DISCUSSIONS

Identical HEMT structures have been grown on two different substrates namely sapphire and silicon (**Fig. 1**) by PAMBE equipped with N_2 RF plasma source. The buffer layers for the HEMTs on silicon (111) comprised of thin AlN nucleation layer, GaN/AlN stack, and a thick GaN buffer. Alternately, in the buffer structure for the HEMTs on sapphire (0001), a thicker AlN nucleation layer along with a single thick GaN buffer was used. Undoped 20 nm AlGaN barrier layer in both structures were capped with a 2nm thin GaN layer. The complete growth methodologies are described elsewhere [6]. Two fingered HEMTs with gate widths and lengths of 50 and 2 µm respectively were fabricated by conventional device processing steps of mesa isolation, ohmic contact formation, and Schottky gate patterning by UV lithography, blanket metal deposition, and liftoff. Notably, no passivation schemes were employed in fabrication so as to thoroughly examine the characteristics of the surface states as well.

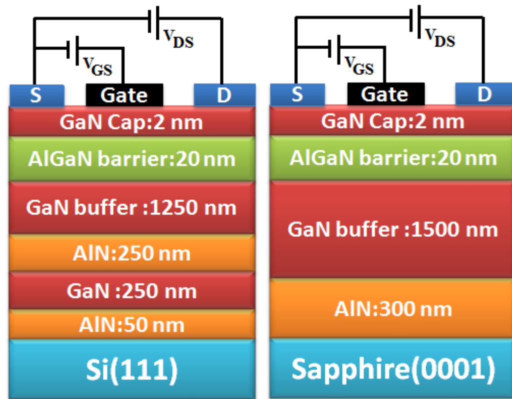

Figure 1.Representative epitaxial structures of the HEMTs grown on silicon and sapphire.

Estimation of the dislocation densities in respective samples were evaluated from TEM and tapping mode AFM imaging. Cross sectional TEM specimens were prepared by standard techniques of ultrasonic disc cutting, mechanical grinding, polishing, and Ar+ ion milling at 3kV up to electron transparency. TEM investigations were performed in a PHILIPS CM-12 microscope operated at 200 kV. For the epitaxial structure grown on silicon, count and nature of the dislocations were determined from **g.b** analysis where **g** and **b** are respectively the diffraction vector, and dislocation burger vector. Two beam bright field images with **g**$=<0002>$ projected most dislocations out of contrast whereas they were in contrast for **g**$=<11\bar{2}0>$ orientations (**Fig. 2**). This concluded that majority of the dislocations were of either pure edge or mixed edge/screw nature. Also, 0.5 μm above the back AlN/GaN interface, the TDDs in the GaN buffer layer were found to be nearly constant, and the dislocation density from directional trace analysis was in the order of $\sim 10^{10}/cm^2$. Furthermore, high resolution AFM (by Agilent N9410S) surface observations were carried out on the structure on sapphire prior to device fabrication. In **Fig. 3**, the $3 \times 3\ \mu m^2$ AFM image of the specimen with typical height index shows step-terrace structure associated with

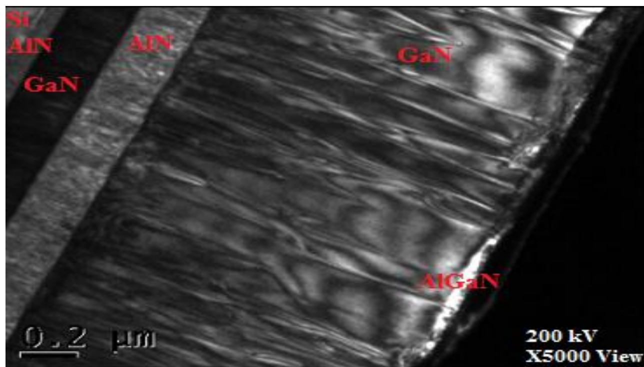

Figure 1. Two beam bright field cross sectional imaging of the device layers grown on silicon showing a dislocation density in the order of $10^{10}/cm^2$.

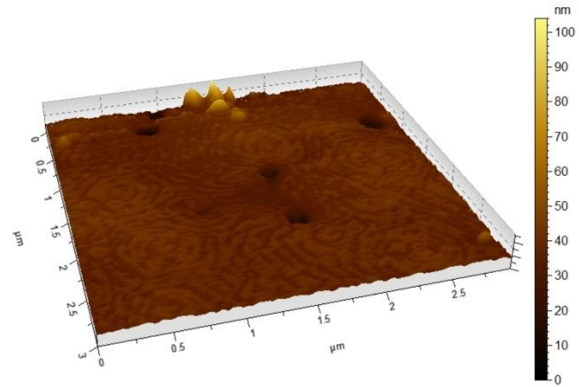

Figure 3.Typical 3x3 μm^2 AFM images of the GaN surface showing a combination of edge and screw dislocations and a cumulative density in the order of 10^8 /cm^2 .

step flow growth of GaN on sapphire along with surface depressions with pit diameter of ~100 nm. Of these, the ones evolving at the termination of the steps are linked with pure/mixed screw dislocations whereas smaller random depressions represent edge type dislocations. The dislocations density for the sapphire sample was significantly lower ($\sim 10^8/cm^2$) than the silicon sample.

Pulsed I-V measurements provide preliminary assessment on trapping effects, and can be approximated as a representation of large signal power performance. Both the DC and pulsed on-wafer characterizations were conducted in a Keithley 4200 SCS in common source configuration. For pulsed measurements, devices were probed with synchronized gate and drain pulses from various bias conditions to study the location and nature of the traps. Four different bias conditions, unstressed (Si:V_{DS}=0V,V_{GS}=0V; Sapphire: V_{DS}=0V,V_{GS}=0V), mild OFF-state stress (Si:V_{DS}=-0V,V_{GS}= -7V; Sapphire: V_{DS}=0V,V_{GS}= -6V), deep ON-state stress (Si:V_{DS}=-10V,V_{GS}=0V; Sapphire: V_{DS}=10V,V_{GS}=0V), and deep OFF-state stress (Si:V_{DS}=-10V,V_{GS}=-7V; Sapphire:V_{DS}=10V,V_{GS}=-6V) were implemented for the measurements. The maximum V_{DS} was kept below 10 Volts for both samples to avoid any permanent defect degradation, and pulse ON-time was fixed at 5 ms for all the four duty cycles (1%,5%,10%, 50%) to eliminate self-heating effects. **Fig. 4** and **5** shows pulsed I-V responses for representative devices from both wafers for 10% duty cycle measurements. Evidently, unpassivated HEMTs grown on silicon showed severe current compression for all bias points particularly with significant increase in knee voltage and as much as 30% current collapse at V_{DS}=8V,V_{GS}=0V for deep OFF-state bias as compared to DC conditions. On the other hand, HEMTs on sapphire suffered no considerable current collapse for all bias conditions. The lagging recovery response of the pulsed currents even for fairly large conduction periods signifies the

presence of deep levels in both the surface/barrier and the buffer of the HEMTs on Si.

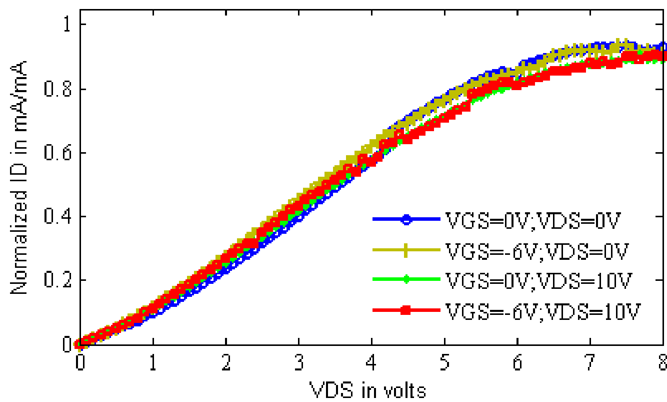

Figure 4. Normalized pulsed I-V data for the HEMT devices on sapphire showing no current collapse when probed from various bias points with 10% duty cycle.

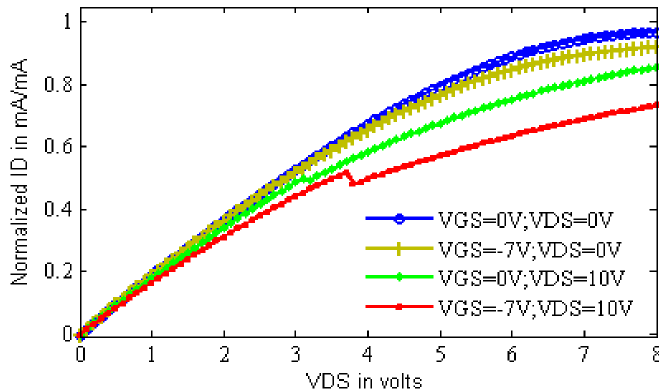

Figure 5. Normalized pulsed I-V data for the HEMT devices on silicon showing severe current collapse when probed from various bias points with 10% duty cycle.

The generalization of the findings were confirmed by using different sequence of bias states for the HEMTs and allowing sufficient restoration time to normal state.

To extract signature time constants of the traps (corresponding to deep levels)we have adapted the technique

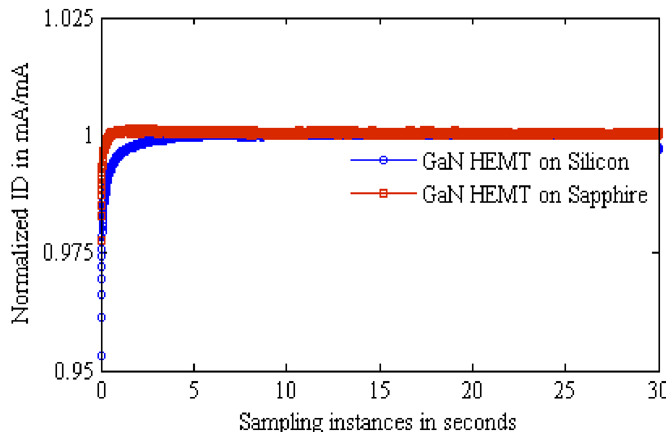

Figure 6. Normalized detrapping current transient for HEMT devices sampled after a deep ON-state pulse.

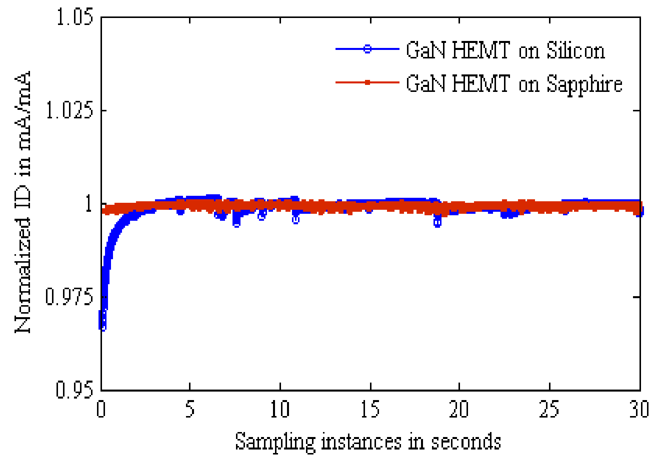

Figure 7. Normalized detrapping current transient for HEMT devices sampled after a deep OFF-state pulse.

developed by [7] which is compatible with stress degradation and reliability tests. Emission time constants extracted from detrapping transient characteristics can be used to analyze different trap levels quantitatively. Accordingly, drain current transients for the devices were measured at V_{DS}=-3V,V_{GS}= -1V for HEMTs on sapphire and at V_{DS}= -3V,V_{GS}=0V for HEMTs on silicon by sampling the drain current at finite time intervals after applying a 1-s long filling pulse simultaneously both at the gate and the drain. During the application of bias pulses, both deep OFF-state bias (V_{DS}=-8V,V_{GS}= -6.5V) and deep ON-state bias (V_{DS}=-10V,V_{GS}=1V) were applied (**Fig. 6** and **7**). At high OFF-state bias, only electron injection occurs from the gate to the drain through the states at the surface whereas in the high on-state bias, current is conducted through both the channel and buffer regions. Thus, implemented bias conditions helped us explore trapping phenomenon on the surface, and also in the channel and the buffer region. To extract the emission time constants of the traps, detrapping I_D transient data were fitted by least square approach with numerical non-linear based finite differencing algorithm to a sum of exponentials with time constants equally spaced logarithmically ranging from one ms to 100 s.

$$I_D(transient) = a_0 + a_1 \exp(-t/\tau_1) + a_2 \exp(-t/\tau_2) + ... + a_n \exp(-t/\tau_n) \quad (1)$$

The total number of coefficients (a_i) was optimized for minimal computing time as well as for accurate relative amplitude and position of time constants. The as computed trap emission time constants for devices on both silicon and sapphire are plotted along with their position and relative amplitudes revealing the involvement of several trapping phenomenon. The constructed detrapping time constant spectrum in **Fig. 8** after a deep-ON state pulse (when trapping occurs in the buffer having high TDDs) shows a

broad peak at ~ 4s for HEMTs on Si among other peaks. In contrast, no peaks with such large time constant was observed for the HEMTs on sapphire. Furthermore, a similar prominent peak was also present in the transient from deep-OFF state (when trapping occurs in the deep states created by surface depression of TDDs) for the HEMTs on Si, and again no such noteworthy detrapping process could be identified for devices on sapphire as shown in **Fig. 9** .

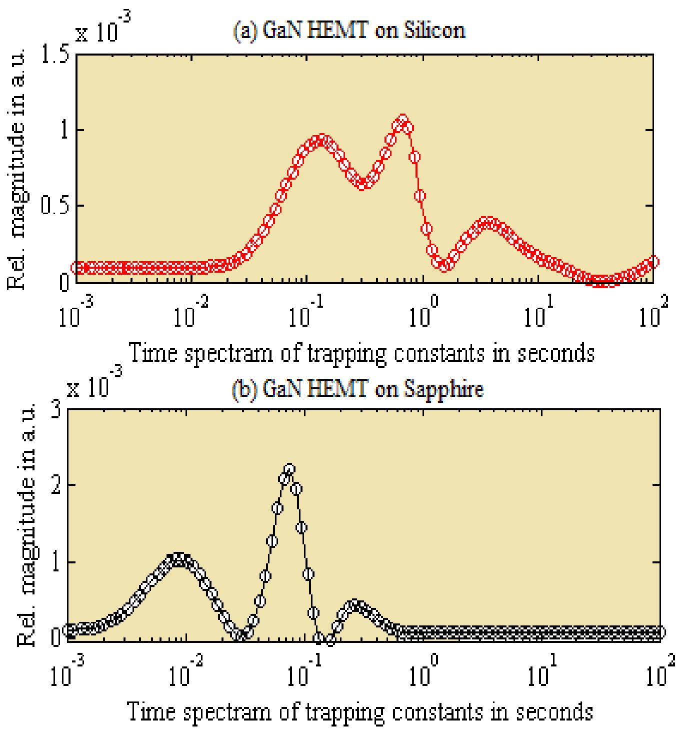

Figure 8. Emission time constant spectra analyzed from detrapping transient after a deep ON-state pulse.

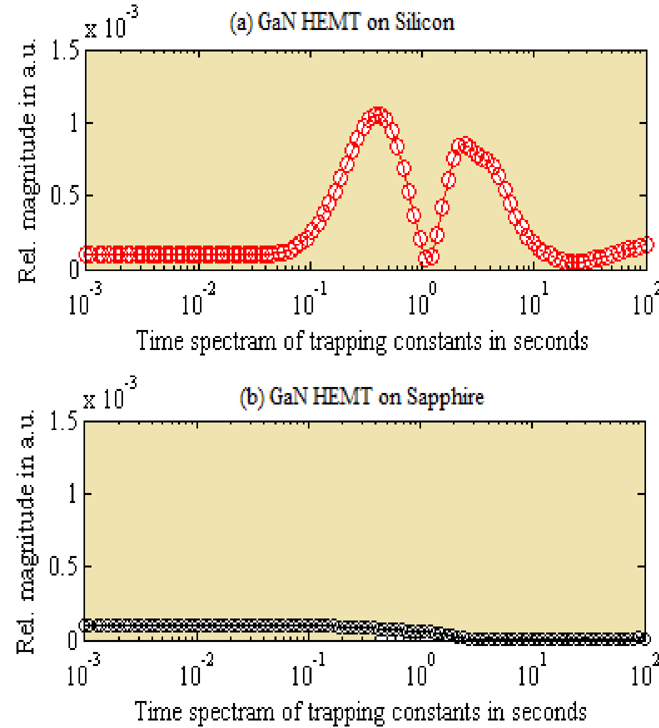

Figure 9. Emission time constant spectra analyzed from detrapping transient after a deep OFF-state pulse.

CONCLUSIONS

In conclusion, the transient performance and pulsed response of AlGaN/GaN HEMTs has been correlated with the dislocation density in the epi-layers. HEMTs grown on Si were found to posses TDDs two orders higher than those on sapphire. The pulsed I-V characteristics for the former suffered severe current collapse indicating trapping phenomenon both at the surface and at the bulk originating from deep levels traps. The signature time constant spectrums extracted from the detrapping transient induced after filling pulses also exhibited the presence of a trap with emission constant in the order of seconds. Shallow point defects and impurities in GaN cannot be accountable for such characteristics. Also, as amplified pulsed current collapse and increased relative trap density is found to be proportionate with increased TDDs, hence slow transient responses for AlGaN/GaN HEMTs on Si can certainly be attributed to electrically active dislocations. In contrast, far less number of TDDs for HEMTs on sapphire was unlikely to affect the transient and pulse response which were indeed observed from the experimental measurements.

ACKNOWLEDGEMENTS

The authors of would like to acknowledge ENS Project, Department of Information Technology (DeitY), Govt. of India for the financial assistance.

REFERENCES

[1] T. Mizutani et al., IEEE Transactions on Electron Devices, 50, pp. 2015-2020 (2003).

[2] J. C. Brooksby et al., Applied physics letters, 90, p.231901 (2007).

[3] K. Shiojima et al., Journal of Vacuum Science & Technology B, 21, pp.698-705 (2003).

[4] D.W. DiSanto et al., Appl. phys. lett., 88, p. 013504 (2006).

[5] L. Lymperakis et al., Physical review letters, 93, p.196401 (2004).

[6] P. Mukhopadhyay et al.,Journal of Electronic Materials, pp.1-8 (2014).

[7] J. Jungwo et al., IEEE Transactions on Electron Devices, 58, pp. 132-140 (2011).

ACRONYMS

HEMT : High Electron Mobility Transistor
TDD : Threading Dislocation Density
HBT : Heterostructure Bipolar Transistor
PAMBE : Plasma Assisted Molecular Beam Epitaxy
TEM : Transmission Electron Microscopy
AFM : Atomic Force Microscopy
DC : Direct Current